We are IntechOpen, the world's leading publisher of Open Access books Built by scientists, for scientists

4,800
Open access books available

122,000
International authors and editors

135M
Downloads

Our authors are among the

154
Countries delivered to

TOP 1%
most cited scientists

12.2%
Contributors from top 500 universities

CLARIVATE ANALYTICS BOOK CITATION INDEX INDEXED

WEB OF SCIENCE™

Selection of our books indexed in the Book Citation Index in Web of Science™ Core Collection (BKCI)

Interested in publishing with us?
Contact book.department@intechopen.com

Numbers displayed above are based on latest data collected.
For more information visit www.intechopen.com

Chapter 9

Role of Modern Localised Electrochemical Techniques to Evaluate the Corrosion on Heterogeneous Surfaces

R. Leiva-García, R. Sánchez-Tovar,
C. Escrivà-Cerdán and J. García-Antón

Additional information is available at the end of the chapter

http://dx.doi.org/10.5772/57204

1. Introduction

Corrosion is a great problem in a lot of chemical industries and in the systems of energy production. When metals are exposed to an aggressive environment or to atmosphere effects tend to reverse to the lesser energy state of ore. All these processes are enhanced by the aggressive conditions that sometimes can be found in the industry, high temperature and pressure or corrosive environments. Therefore, corrosion may imply a lot of economic costs in the productive system. According to NACE [1] in 2002 the cost of corrosion in USA could be established in 276 million of dollars per year. Therefore, it is quite important to develop and use techniques that can allow determining and monitoring the corrosion of the metals.

Since 1903, when the electrochemical character of corrosion was widely accepted after the publication of the paper of Whitney [2], several electrochemical techniques has been developed and used in the study of the corrosion processes. Some of the main milestones developed in the electrochemistry science during the 20th century can be summarised as follows:

1. Alexander Naumovich Frumkin (1895-1976). made vital contributions to our knowledge of the fundamentals of electrode reactions — particularly the influence of the electrode-electrolyte interface on the rate of electron transfer across it [3].
2. Veniamin Grigorevich Levich (1917-1987), an associate of theoretical physicist Lev Davidovich Landau (1908-1968), helped Frumkin in relating his experimental results to theory. The collaboration led to the development of the rotating disc electrode [4].
3. The quantitative measurement of electrochemical corrosion got established with a 1932 publication of Thomas Percy Hoare (1907-1978) and Ulick Richardson Evans (1889-1980).

His 1937 book "Metallic Corrosion, Passivity, and Protection" is probably one of the clearest books written on corrosion science.

4. 1938, the Belgian electrochemist Marcel Pourbaix (1904-1998) constructed his famous potential–pH diagrams "Pourbaix diagrams".

5. Much of the theory behind cyclic voltammetry and electrochemical impedance spectroscopy came from the work of the English electrochemist John Edward Brough Randles (1912-1998).

6. One important development in electrochemical instrumentation is the invention of the potentiostat by the German engineer-physicist Hans Wenking (1923).

Nowadays, electrochemistry and corrosion science looks interconnect with parallel advancements in materials science and characterization techniques. For example, there is increasing thrust toward exploiting nanoscopic materials and architectures. Expectations in this direction are high because surface plays a key role in electrochemical processes. Continual developments in the synthesis and characterization of materials have also led to welcome changes in electrochemical research.

Therefore, the use of the electrochemical techniques has demonstrated being quite helpful in the study and control of corrosion in several environments. In this chapter a review of the conventional and localised electrochemical techniques applied to the analysis of corrosion processes has been made. Additionally, some experimental results of the authors, which are a good example of the use of localised electrochemical techniques in the study of heterogeneous materials, are presented.

2. Stainless steels

Stainless steel is a generic name commonly used for that entire group of iron-based metal which are the most commonly used metallic materials. The main characteristics are their resistance to corrosion in many environments, their good mechanical properties over an extremely wide range of temperatures and their resistance to oxidation and scaling at very high temperatures [5, 6]. These compounds contain at least a 12% of chromium, low carbon content and they might also have percentages of other elements such as nickel, molybdenum, vanadium, titanium, aluminium and so on. The corrosion resistance of stainless steels is provided by a very thin and protective surface oxide film, known as passive film. It is generally accepted that passive films formed on stainless steels have a duplex structure which consists of an inner region rich in chromium and an outer region rich in iron [7-10]. Nickel and molybdenum are commonly added in the stainless steel composition in order to increase its corrosion resistance.

There are five main classes of stainless steel: austenitic stainless steels, martensitic stainless steels, ferritic stainless steels, duplex stainless steels and precipitation hardening stainless steels.

http://dx.doi.org/10.5772/57204

2.1. Austenitic stainless steels

Austenitic stainless steels are the most common and familiar types of stainless steel. They are not magnetic. They have a face-centred-cubic lattice structure of austenite over the whole temperature range from room temperature (and below) to the melting point. The austenitic stainless steels, because of their high chromium and nickel content, are the most corrosion resistant of the stainless group. Moreover, they are weldable and can be divided into three groups: common chromium-nickel (300 series), manganese-chromium-nickel-nitrogen (200 series) and specialty alloys. The commonly used austenitic alloys contain chromium (17-27 wt. %), nickel (6-32 wt. %) and low carbon amounts (0.02-0.1 wt. %) in an iron matrix. Austenitic stainless steels are used for numerous industrial and consumer applications, such as in chemical plants, power plants, food processing equipment [11].

The most common austenitic grades are the 304 and the 316 ones [12]. Austenitic 304 grade contains approximately 18 wt. % of chromium and 8 wt. % of nickel contents. This kind of stainless steel is widely used for chemical processing equipment, for food, dairy, and beverage industries, for heat exchangers and for the milder chemicals. Type 316 is an austenitic chromium nickel stainless steel containing molybdenum. This addition increases general corrosion resistance, improves resistance to pitting from chloride ion solutions and provides increased strength at elevated temperatures [13]. Properties are similar to those of Type 304 except that this alloy is somewhat stronger at elevated temperatures. Corrosion resistance is improved, particularly against sulphuric, hydrochloric, acetic, formic and tartaric acids, acid sulphates and alkaline chlorides. Table 1 shows the typical composition of an austenitic 304 and 316 grade, respectively [14].

	Type 304	**Type 316**
Carbon	0.08 max.	0.08 max.
Manganese	2.00 max.	2.00 max.
Phosphorus	0.045 max.	0.045 max.
Sulfur	0.03 max.	0.03 max.
Silicon	0.75 max.	0.75 max.
Chromium	18.00-20.00	16.00-18.00
Nickel	8.00-12.00	10.00-14.00
Molybdenum	-	2.00-3.00
Nitrogen	0.10 max.	0.10 max.
Iron	Balance	Balance

Table 1. Composition of type 304 and 316 stainless steels, values are given in wt. %

2.2. Martensitic stainless steels

Martensitic stainless steels are a chromium-iron alloy containing 10.5 to 17 wt %. chromium and controlled amounts of carbon. They are ferromagnetic, hardenable by heat treating, and generally resistant to corrosion only in relatively mild environments. This kind of alloy

is extremely strong and tough, as well as highly machinable. The martensitic grades are mainly used where hardness, strength, and wear resistance are required, i.e. they are specified when the application requires good tensile strength, creep and fatigue strength properties, in combination with moderate corrosion resistance and heat resistance up to approximately 650 °C [15].

The most commonly used alloy within the martensitic stainless steel family is type 410, which contains approximately 12 wt% Cr and 0.1 wt% C to provide strength. It is widely used where corrosion is not severe (air, water, some chemicals, and food acids). Typical applications include highly stressed parts needing the combination of strength and corrosion resistance such as fasteners.

2.3. Ferritic stainless steels

Ferritic stainless steel grades contain between 10.5 wt % and 27 wt % chromium and very little nickel, if any, but some types can contain lead. Most compositions include molybdenum; some, aluminium or titanium. They were developed to provide a group of stainless steel to resist corrosion and oxidation, while being highly resistant to stress corrosion cracking [16, 17]. These kind of alloys are magnetic but cannot be hardened or strengthened by heat treatment, as martensitic grades. They can be cold worked and softened by annealing. As a group, they are more corrosive resistant than the martensitic grades, but generally inferior to the austenitic grades. The basic ferritic grade is type 430, with a little less corrosion resistance than type 304. Type 430 combines high resistance to such corrosives as nitric acid, sulfur gases and many organic and food acids.

2.4. Duplex stainless steels

Duplex stainless steels have a mixed microstructure of austenite and ferrite and roughly twice the strength compared to austenitic stainless steels. They also have improved resistance to localized corrosion, particularly pitting, crevice corrosion and stress corrosion cracking. They are characterized by high chromium (19–32 wt %) and molybdenum (up to 5 wt %) and lower nickel contents than austenitic stainless steels. That is why they have lower cost [18, 19]. Duplex stainless steels are considered a very attractive structural material in the field of energy/environmental systems due to their good mechanical and corrosion resistance properties. However, the higher Cr and Mo content in duplex stainless steels can promote the precipitation of secondary phases, such as sigma phase [20, 21]. These phases, which are rich in alloying elements, appear when the steel is heated in a specific range of temperatures. During these heat treatments, the microstructure of duplex stainless steels undergoes morphological changes. The ratio of the ferrite and the austenite phase, that in the beginning is 1/1, changes with the heat treatment temperature. Duplex stainless steels are typically used in the main following areas: chemical processing, transport and storage; oil and gas exploration and offshore rigs; oil and gas refining; marine environments; pollution control equipment; pulp and paper manufacturing and chemical process plants.

http://dx.doi.org/10.5772/57204

2.5. Precipitation hardening stainless steels

Precipitation hardening grades are iron-nickel-chromium alloys containing one or more precipitation hardening elements such as aluminum, titanium, copper, niobium, and molybdenum. The two main characteristics of all precipitation-hardening stainless steels are high strength (at the expense of toughness) and high corrosion resistance (comparable to that of the standard 304 and 316 austenitic alloys) [22]. The aging treatments are designed to optimize strength, corrosion resistance, and toughness. On the other hand, to improve toughness, the amount of carbon is kept low.

3. Generation of heterogeneous surfaces in stainless steels

Welding is widely used in the fabrication, maintenance, and repair of many industrial parts and structures, especially for the joint of stainless steels. However, welding introduces residual stresses into the material and can cause cracking as the weld cools and contracts. Minor differences in composition and microstructure between a weld and a base zone can create an electrochemical potential between the zones and may cause galvanic corrosion [23]. In fact, corrosion in welds has always been a problem due to local variations in material composition and structure. When austenitic stainless steels are incorrectly heat treated, in the temperature range between 500 and 900 °C, chromium and carbon combine at the grain boundaries to form chromium carbides (typically $Cr_{23}C_6$), whilst simultaneously as these carbides form, chromium depletion occurs at the adjacent zones. This process is called sensitisation and leads to a decrease in the corrosion resistance of stainless steels, notably resistance to intergranular corrosion, being due to the depleted regions becoming anodic in the presence of an electrolyte [24-30]. These heat treatments generate heterogeneous surfaces on the stainless steels. The "L" grades are used to provide extra corrosion resistance after welding. The letter "L" after a stainless steel type indicates low carbon (as in 304L). The carbon is kept to 0.03 wt. % or under to avoid carbide precipitation [31]. The most common grade L stainless steel types are 304L and 316L. In this way, the welding procedure itself or the generation of sensitization zones in stainless steels due to welding or heat treatments create heterogeneities in the alloy, which might lead to corrosion problems or contribute to aggravate them. For this reason, the electrochemical study of these materials is a very important issue. All these corrosion mechanisms have mainly been studied using 'macro' experiments (working electrode in the mm^2 – cm^2 range) [32, 33]. However, such processes are due to mechanisms on a smaller scale. Therefore, it is beneficial to develop appropriate 'micro' experimental devices that require a reduced working electrode surface area [34]. In this context, microelectrochemical methods are powerful techniques to study localised corrosion processes on small areas of passive metals, microgalvanic cells, etc [35-37].

4. Conventional techniques in the study of stainless steels

Corrosion science and engineering have benefit tremendously from the use of electrochemical methods that can probe the thermodynamic and kinetic aspects of corrosion, including the rate

of corrosion. These methods have proved of great utility to corrosion engineers and scientists in predicting the performance of materials and devising corrosion mitigation strategies, understanding the effects of changes in process and environment conditions, and assessing the accuracy of corrosion monitoring techniques [38]. Some of the most common techniques used in research studies are described in the following sections.

DC electrochemistry, and in particular, the potentiodynamic polarisation scan, is a rapid method of obtaining an insight into the corrosivity of a particular environment for a steel. Through the DC polarisation technique, information on the corrosion rate, pitting susceptibility, passivity, as well as the cathodic behaviour of an electrochemical system may be obtained.

In a potentiodynamic experiment, the current represents the rate with which the anodic and cathodic reactions are taking place on the working electrode. Typically, the current is expressed in terms of the current per unit area of the working electrode, or the current density. Numerous variables will influence the rate of a given electrochemical reaction, including the temperature, the surface condition of the surface being interrogated, as well as the chemical environment in which the experiment is performed. In this experiment, the driving force (i.e., the potential) for anodic and cathodic reactions is controlled, and the net change in the reaction rate (i.e., current) is observed.

The reaction rate may be controlled by two different kinetic phenomena. The first is charge transfer or activation control. In this case, the reaction is controlled by the size of the driving force available (e.g., hydrogen evolution reaction or water reduction reaction). As the driving force increases, so does the reaction rate. The other mechanism which may control the reaction rate is mass transfer. In this case, the reaction rate is controlled by mass transfer through the electrolyte to the electrode surface (e.g., oxygen reduction reaction). Since the reaction rate is controlled by diffusion, it cannot increase indefinitely as the driving force increases. Instead, the current reaches a maximum, or limiting, current density which is itself a function of the concentration of the species of interest in the solution as well as its diffusivity. Once the rate for a particular reaction has reached its limiting value, further increases in driving force will not result in any additional increase of the reaction rate [39, 40].

During the potentiodynamic polarisation scan, the potential of the electrode is controlled, while the current is determined as a function of time. The opposite case, where the current is controlled (frequently held constant), and the potential becomes the dependent variable, which is determined as a function of time. The experiment is carried out by applying the controlled current between the working and auxiliary electrodes with a current source (called a *galvanostat*) and recording the potential between the working and reference electrodes (e.g., with a recorder, oscilloscope, or other data acquisition device) (Figure 1). These techniques are generally called *chronopotentiometric techniques*, because E is determined as a function of time, or galvanostatic techniques, because a small constant current is applied to the working electrode [39].

Another DC technique is the ZRA (Zero resistance ammeter), this device is a current to voltage converter that produces a voltage output proportional to the current flowing between its to

http://dx.doi.org/10.5772/57204

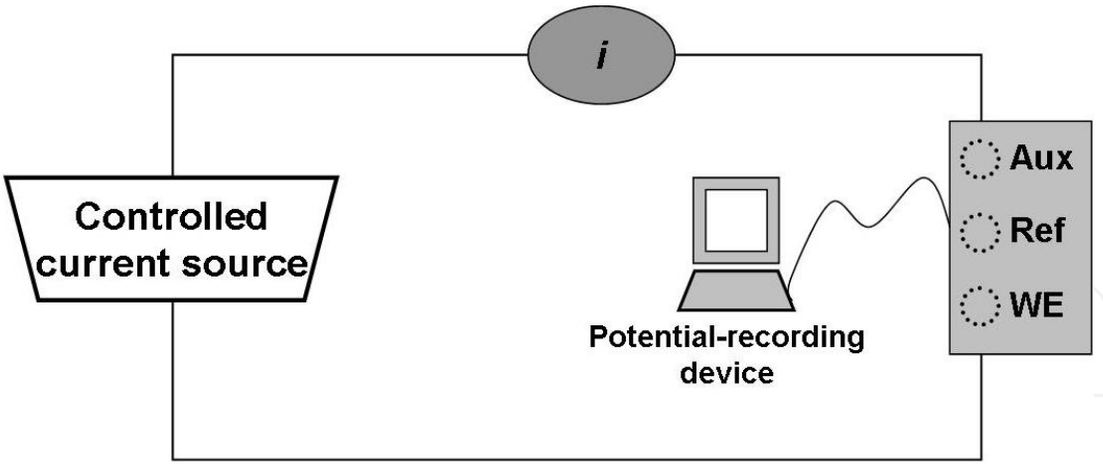

Figure 1. Simplified block diagram of the setup for chronopotentiometric measurements.

input terminals while imposing a 'zero' voltage drop to the external circuit. In corrosion test a ZRA is typically used to measure the galvanic coupling current between two dissimilar electrodes. An interesting application is when the coupling current between two nominally identical electrodes is measured. If both electrodes were identical then very little coupling current would flow. In real situations these electrodes will be slightly different, one being more anodic or cathodic than the other and a small coupling current will exist [41, 42].

On the other hand, *AC impedance methods* are widely used for the characterisation of electrode processes and complex interfaces. These methods are commonly called Electrochemical Impedance Spectroscopy (EIS) and study the system response to the application of a periodic small amplitude AC signal. These measurements are carried out at different AC frequencies and, thus, the name impedance spectroscopy was later adopted. Analysis of the system response contains information about the interface, its structure and reactions taking place there. EIS is now described in the general books on electrochemistry and specific books [39], and there are also numerous articles and reviews [43-46]. It became very popular in the research and applied chemistry [47].

5. Localised techniques in the study of stainless steels

Once the generalised techniques have been presented, a brief summary of the available localised electrochemical techniques is presented, indicating the principles and main applications of each of them.

5.1. Scanning electrochemical microscopy (SECM)

Scanning electrochemical microscopy has become a powerful technique for quantitative investigations of interfacial physicochemical processes, in a wide variety of areas, as considered in several reviews [48-50]. In the simplest terms, SECM involves the use of a mobile

ultramicroelectrode (UME) probe, either amperometric or potentiometric, to investigate the activity and/or topography of an interface on a localized scale [51].

Therefore, SECM is based on the possibility of precisely positioning a probe close to the object under investigation (substrate). In the case of SECM, the probe is an ultramicroelectrode, which is an electrode of nanometer to micrometer dimension. Ultramicroelectrode and substrate are both immersed into an electrolyte solution containing either an oxidizable (or reducible) chemical species, which is called mediator. The ultramicroelectrode is electrically biased so that a redox current, the tip-current, is generated. When the ultramicroelectrode is brought near the substrate the tip-current changes and information about the surface activity of the substrate can be extracted. By scanning the ultramicroelectrode laterally above the substrate one can acquire an image of its topography and/or its surface reactivity [51]. Several modes of SECM have been developed to allow the local chemical properties of interfaces to be investigated [51], two of them are the *Feedback Mode* and the *Generation-Collection Mode.*

In the first one (*Feedback Mode*), the species are reduced or oxidised at the tip, producing a steady-state current that is limited by hemispherical diffusion. As the tip approaches to a conductive substrate in the solution, the reduced species formed at the tip is oxidized at the conductive surface, yielding an increase in the tip current and creating a regenerative "positive" feedback. The opposite effect is observed when insulating surfaces are probed, as the oxidized species cannot be regenerated and diffusion to the electrode is inhibited as a result of physical obstruction as the tip approaches the substrate, creating a "negative" feedback loop and decreasing the tip current [52]. One scheme of this effect is presented in Figure 2. However, sometimes the negative feedback is also observed when there is a competitive reaction between the tip and the substrate; this is the case when the oxygen reduction is the followed reaction and the substrate is a stainless steel [53].

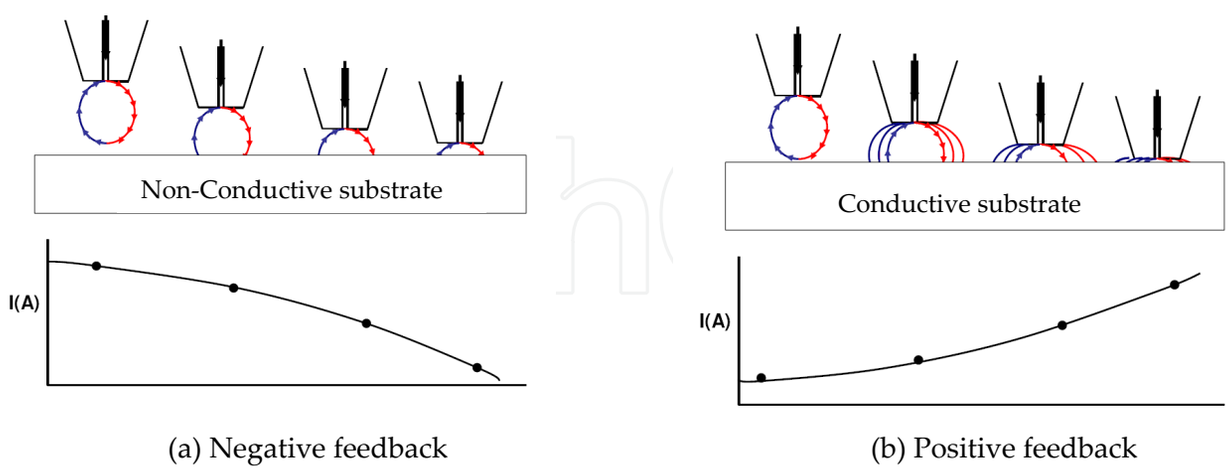

Figure 2. Scheme of the evolution of the current registered on the tip during the feedback mode.

On the other hand, the other modes of operation are the Generation Collection modes. In the Tip generation/substrate collection (TG/SC) mode, the tip is held at a potential sufficient for an electrode reaction to occur and "generate" a product while the substrate is held at a potential

http://dx.doi.org/10.5772/57204

sufficient for the product to react with or be "collected" by the substrate [53]. The reciprocal to this method is the substrate generation/tip collection (SG/TC), where the substrate acts to generate species that are measured at the tip. Both TG/SC and SG/TC variations are also categorized as "direct" modes [51].

Among the main applications of the SECM technique, some of them are: corrosive activity of the tested materials, topographic maps of the samples, measurements of heterogeneous of homogeneous kinetics of reactions, study of the electrochemical behaviour of membranes or surface reactions.

5.2. Scanning droplet cell (SDC)

A new electrochemical device, the capillary-based droplet cell [54, 55] is a technique which confines a liquid in contact with a sample surface in order to measure electrochemical and corrosion reactions over a limited region where the droplet is actually in contact with the sample. This Scanning Droplet Technique provides facilities for micro-electrochemical investigations at high resolution, in which small electrolyte droplets are positioned on the sample surface, enabling a spatially resolved surface analysis or modification. The small area of the working electrode determined by the tip size of a capillary with a diameter of 20–600 μm enables the investigation of localized corrosion or passivation of small areas within a single grain or phase. In addition, the device has a smaller resolution than some special probe techniques (e.g. STM), but enables a complete range of potentiostatic (or dynamic) and galvanostatic (or dynamic) techniques including impedance spectroscopy.

This is accomplished by providing a convenient three-electrode system consisting of the working electrode of interest (the wetted surface area under investigation) and the capillary contains the counter and reference electrodes which are electrically connected to the surface through the drop. The wetted area is approximately determined by the capillary radius. The small distance between the counter electrode and the sample allows high current densities due to the small ohmic resistance. The electrolyte drop is then scanned at high resolution across the surface of the sample.

The scanning droplet system allows a spatially resolved, in-situ investigation by the standard electrochemical techniques such as line scans, area maps, potentiostatic pulse steps and open circuit measurements.

5.3. Scanning Kelvin Probe (SKP)

The Kelvin Probe is a non-contact, non-destructive measurement device used to investigate properties of materials [56;57]. It is a tool with wide applications for both surface science and industrial uses. It is based on a vibrating capacitor and measures the work function difference or, for non-metals, the surface potential, between a conducting specimen and a vibrating tip [58-60]. This method exploits the well-established principles of direct correlation between work function and surface condition. The work function is an extremely sensitive indicator of surface condition and is affected by adsorbed or evaporated layers, surface reconstruction, surface charging, oxide layer imperfections, surface and bulk contamination, etc. [61].

Regarding the operation mode, a metal microprobe is positioned close to the surface of the sample (on the order of 100-microns). If the microprobe and sample are of different metals, there is an energy difference between their electrons. The microprobe is then electrically shorted to the sample, through internal electronics of the system. As a consequence, one metal forms a positive charge on its surface and the other metal forms a negative charge on its surface. The probe and sample are separated by a dielectric (air), so a capacitor is formed. The probe is then vibrated and "backing potential" or "nulling potential" is then applied sufficient to minimize this capacitance. At the applied voltage that causes the capacitance to go to zero, the original state is achieved. This value is recorded and charted. Experiments are typically performed in ambient gaseous conditions, but several published examples use humidified environments.

One improvement of this technique is the Scanning Kelvin Force Microscopy (SKPM) [62-64], this technique allows to measure the local potential between a conducting atomic force microscopy (AFM) tip and the sample. Therefore, with this method it is possible to characterise the nano-scale electronic/electrical properties of metal/semiconductor surfaces and semiconductor devices. Among the main applications of the SKP technique, some of the most important are: study of coatings interfaces, study of galvanic pairs or the oxide formation effect.

5.4. Scanning vibrating electrode technique (SVET)

The scanning vibrating probe electrode measures the potential drop generated by current flow in a small volume of solution by vibrating Pt-Ir tipped microelectrodes between two virtual points in the electrolyte at a defined distance from the surface [65]. In corrosion of metals, this will reflect the distribution of current associated with anodic and cathodic current at the metal surface but with decreasing resolution of local anodic and cathodic processes with distance from the surface and with increasing conductivity of the solution. For the latter reason, relatively low conductivity solutions may be necessary for some systems, sufficient to generate distinguishable potential gradients in solution. Then, the scanning Vibrating Electrode Technique (SVET) uses a scanning microelectrode to measure these gradients in situ, thereby, locating and quantifiying the corrosion activity at specific points on the sample surface. Measurements are made by vibrating a fine tipped microelectrode a few hundred microns about the sample in a perpendicular plane to the surface. The electrochemical potential of the microelectrode is recorded at the extremes of vibration amplitude, resulting in the generation of a sinusoidal AC signal. This signal is then measured using a lock-in amplifier, which is tunned to the frequency of the probe vibration. Furthermore, the resulting signal, which is the effect in effect a measure of the DC potential gradients in solution, can be converted to current density by a simple calibration procedure [66]. This technique is, therefore, able to make in-situ measurements of the localised corrosion activity occurring at the sample surface.

This method was originally devised by biologists for the measurement of extracellular currents near to living cells. Isaacs, later developed the technique to study various localised corrosion processes, including stress corrosion cracking of AISI 304 stainless steels and corrosion inhibition by cerium salts [65]. The main applications of the SVET technique to the material

http://dx.doi.org/10.5772/57204

science are: study of defect evolution in coatings, galvanic study during a corrosion process, evolution of artificial defects or determination of precursor sites for corrosion.

5.5. Localised electrochemical impedance spectroscopy (LEIS)

As previously mentioned, electrochemical impedance spectroscopy (EIS) is an in-situ non-destructive technique, which has been widely employed in the study of corrosion processes, and in particular is now widely accepted as a standard technique for the investigation of corrosion an coatings. However, difficulties arise in EIS, when attempting to study localised electrochemical processes, as impedance is calculated from the bulk current and voltage data, and it is, therefore, averaged across the entire surface area of the sample. In order to make impedance measurements on a local scale, work by a number of authors has been conducted to combine established DC scanning techniques with AC impedance techniques [67, 68], resulting in the evolution of LEIS.

The principles of LEIS are similar to those used in the conventional bulk EIS; a small sinusoidal voltage perturbation is applied to a working electrode sample and the resulting current is measured to allow the calculation of the impedance. However, rather than measure the bulk current from the whole surface area, an electrochemical probe is scanning close to the surface in order to measure the local current distributions in the electrolyte. This probe incorporates two platinum electrodes; one constitutes the tip of the probe and is electrochemically sharpened to approximately 5 mm of diameter and the other is a ring positioned at a distance of 3 mm over the tip. Each of these electrodes is platinised in order to increase the active area and therefore, to reduce the interfacial area between the electrode and the electrolyte. The potential difference between both platinum electrodes is measured via an electrometer and, for known solution conductivity, the local current is calculated. Then the ratio between the AC perturbation applied to the sample and the local current density determine the local impedance. Therefore, this approach gives spatial resolution to the measurement of the electrochemical impedance, overcoming the limitations of the surface averaging encountered in the conventional EIS measurements [69, 70].

5.6. Scanning refererence electrode technique (SRET)

Scanning reference electrode technique (SRET) is an in situ technique used to study the electrochemical process during localized corrosion without interrupting the process taking place. Within the electrolyte directly above a localized electrochemical active site, there exists an electromagnetic field. A probe consisted of two platinum wires can sense the potential difference between two different places where the two platinum wires are located. This potential difference then is processed by a differential amplifier. By scanning the SRET probe over the surface of the test material immersed in an electrolyte, these fields may be mapped out as a function of x and y or monitored with respect to time. Resulting data can be instantly display, stored and manipulated in a number of formats including individual linescans, area maps and sequential time related images.

The potential field distribution over the surface of the electrochemically active site is representative of the localized current flow. By using a calibration procedure the SRET can also be used to make discrete current measurements.

5.7. Summary

Once the main principles of the localised electrochemical techniques have been presented in the previous point, an overview of the current application of these techniques to the study of heterogeneous surfaces will be commented. Three different kind of studies will be taken into consideration:

5.7.1. Coatings and protective films

One way to protect metals from corrosion is the use of protective films such as coatings. These films can undergo defects that can decrease their functionality. The use of the localised electrochemical techniques can be quite helpful to study the behaviour of these defects. Kinlen [71] used the SRET technique in order to analyse the effect of conductive polymers such as polyaniline (PANI) in the use of coatings formulations and which was the its toleration to minor scratches. This technique has been also used by several authors to study different sort of coatings, such as PVD ceramic-coated steels [72], or physical vapour deposition (PVD) coated samples [73]. Other way to study the local defects on coatings is the SECM technique, with this technique is possible to evaluate the electrochemical activity that surrounds a defect or the initial points where corrosion begins. Examples of that are: the studies of the cathodic protection of aluminium by means of a magnesium coating conducted by Simoes [74, 75] or the studies of damage to paint coatings carried out by Souto [76, 77]. On the other hand, using the SVET or the LEIS devices it is also possible to evaluate the cathodic and anodic sites that appears in the coatings when samples are immersed in an electrolyte, some conducted studies are: the study of microdefects on a coated AZ31 magnesium alloy [78], the observation of self-healing functions of galvanised steel [79] or the evaluation of the PEO-coating/substrate interface [80]. Finally, also the Scanning Kelvin probe can be used in order to study electrochemical differences between coated and uncoated metals[81].

5.7.2. Welds and sensitised samples

As it has been explained previously, when the microstructure on an alloy changes as a consequence of a heat treatment, the corrosion properties change too. Therefore, it is very useful the use of the localised electrochemical techniques in order to evaluate the local electrochemical behaviour. Microcell techniques, with a similar configuration to the Droplet cell have been widely used to determine the properties of the different parts of a weld specimen. One example of this is the cell developed by García in order to study the weld behaviour in AISI 304 and 316L [34]. On the other hand, other authors prefer a different approach to the problem using the SECM system. Some of the most relevant studies carried out are: visualization of local electrochemical activity and local nickel ion in weld Ni/Ti steels [82], characterisation of the electrochemical activity at the interface of a dissimilar explosive joint of stainless steel [83], evaluation of the effects of microplasma arc AISI 316L welds [84]

or the study of the sensitisation of a highly alloyed austenitic stainless steel [53]. In the same way, the SVET technique can be used in the study of welds on order to determine the anodic and the cathodic sites of the heated samples. One example of that is the investigation into the effect of a spot weld electrode using 3-D SVET [85] conducted by Benjamin in 2012.

5.7.3. Identification of anodic and cathodic sites

Finally, all the localised electrochemical techniques can be used to determine the anodic and cathodic distribution on the surface of the tested samples or the areas that are more susceptible to corrosion, showing higher current density or lower potential. An example of this kind of work is the visualisation of pits by means of the SECM technique [86-88]. In this way it is possible to evaluate the points where the localised corrosion will begin. On the other hand, these cathodic and anodic areas or their activity can be determined using the Scanning Vibrating Electrode or Localised Impedances, the first one allows to establish the anodic and cathodic areas or study inclusions [89, 90]; the second one permits analysing the admittance of the metal/electrolyte interphase in the different areas [91]. Furthermore, when metals with different characteristics are coupled, the galvanic activity can be determined. Simoes used the SECM and the SVET system to determine the galvanic properties of an iron-zinc cell, observing that both techniques has a comparable sensibility [92].

Table 2 presents different papers and communications where the localised techniques are used to study corrosion in metallic materials:

Authors	Journal	Research topic	Technique
Jean-Baptiste et al.	Corrosion Science 48 (2006) 1779–1790	Delaminated areas beneath organic coating: A local electrochemical impedance approach [93]	LEIS
Z.Y. Liu et al.	Electrochimica Acta 60 (2012) 259– 263	Understand the occurrence of pitting corrosion of pipeline carbon steel under cathodic polarization [94]	LEIS
Darya Snihirova et al.	Electrochimica Acta, In Press	"SMART" protective ability of water based epoxy coatings loaded with CaCO3 microbeads impregnated with corrosion inhibitors applied on AA2024 substrates [95]	LEIS
Halina Krawiec et al.	Electrochimica Acta 53 (2008) 5252-5259	Numerical modelling of the electrochemical behaviour of 316 stainless steel based upon static and dynamic experimental micro-capillary based techniques: effects of electrolyte low and capillary size [96]	SDC
S. Gnefid, R. Akid	The European Corrosion Congress 2009	The Effects of Flow Rate on Pitting Corrosion of DSS2205 [97]	SDC
Leiva García et al.	Electrochimica Acta, 70, 2012, pp 105-111	Study of the sensitisation of a highly alloyed austenitic stainless steel, Alloy 926 (UNS N08926), by means of scanning electrochemical microscopy [53]	SECM
Yawei Shao et al.	Corrosion Science 51 (2009) 371–379	The role of a zinc phosphate pigment in the corrosion of scratched epoxy-coated steel [98]	SECM

Authors	Journal	Research topic	Technique
Yuehua Yin et al.	Applied Surface Science 255 (2009) 9193–9199	In situ characterization of localized corrosion of stainless steel by scanning electrochemical microscope [99]	SECM
Xiaolan Liu et al.	Corrosion Science 51 (2009) 1772–1779	Effect of alternating voltage treatment on the corrosion resistance of pure magnesium [100]	SECM
A.Q. Fu et al.	Corrosion Science 51 (2009) 914–920	Characterization of corrosion of X65 pipeline steel under disbonded coating by scanning Kelvin probe [101]	SKP
A.Q. Fu et al.	Corrosion Science 51 (2009) 186–190	Characterization of corrosion of X70 pipeline steel in thin electrolyte layer under disbonded coating by scanning Kelvin probe [102]	SKP
Cavalcolid et al.	Journal of the Electrochemical Society. Vol. 150, G456-G460 2003	Surface contaminant detection in semiconductors using noncontacting techniques. [103]	SKP
K.Borgwarth et al.	Electrochimica Acta, Jul 1995	Applications of scanning ultra micro electrodes for studies on surface conductivity [104]	SRET
I.M. Zin et al.	Progress in organic coatings 2005, 52, 126-135	Under-film corrosion of epoxy-coated galvanised steel an EIS and SVET study of the effect of inhibition at defects [105]	SVET
Kiran B	Electrochimica Acta 56 (2011) 1737–1745	Numerical modeling of micro-galvanic corrosion [106]	SVET
Francois Berger et al.	Electrochimica Acta, volume 53, 2010, 2852-2861	Hybrid coating on steel: ZnNi electrodeposition and surface modification with organothiols and diazonium salts [107]	SVET
G.A. Zhang, Y.F. Cheng	Corrosion Science 51 (2009) 1714–1724	Micro-electrochemical characterization of corrosion of welded X70 pipeline steel in near-neutral pH solution [108]	SVET & LEIS
R. Akid et al.	Local Probe Techniques for corrosion research. 978-1-4200-5405-7 (CRC Press)	Application of scanning vibrating electrode technique (SVET) and scanning droplet cell (SDC) techniques to the study of weld corrosion [109]	SVET & SDC

Table 2. Research studies where localised electrochemical techniques are applied to the study of materials.

6. Applications of localised techniques in the study of heterogeneities in stainless steels

After presenting the different localised electrochemical techniques and the main application of then to different heterogeneous surface, two different applications of localised techniques conducted in the "Ingeniería Electroquímica y Corrosión" group from the Universitat Politècnica the València will be explained. The first one corresponds to some experiments carried out with a duplex stainless steel under different sensitisation conditions. The second one, correspond to the evaluation of the local electrochemical properties of a weld in AISI 316L.

http://dx.doi.org/10.5772/57204

6.1. Sensitisation process in a duplex stainless steel

Conventional electrochemical techniques have been widely used to study sensitisation and provide important information about the sensitisation processes on steels [25, 27, 29, 30]. In contrast to pure metals, alloys have rarely been investigated using the micro-droplet cell because of their complexity in structure and chemical composition. Duplex stainless steel (Alloy 900) is potentially a good candidate for micro-electrochemical investigations with the droplet cell, because this alloy is composed of an approximately equal volume fraction of ferrite (α) and austenite (γ) phase, and, sometimes, secondary phases such as sigma (σ) or alpha prime (α') phase [20, 110, 111]. Figure 3 shows the SEM micrographs of Alloy 900 after different heat treatments in an inert atmosphere; these images were obtained using backscattered electrons. In the images it can be observed the change in the percentage of the present phases and the formation of new intermetallic phases such as sigma and chi.

The advances in the field of localised microelectrochemical techniques have provided the facility to acquire spatially resolved information about the corrosion processes occurring on the surface of the metal. The Scanning Droplet cell and the Scanning Electrochemical Microscopy have been used to evaluate the effect of the sensitisation on the electrochemical behaviour of the samples.

In order to conduct the tests with different samples of Alloy 900 at the same time, individual unsensitised and sensitised samples were mounted in epoxy resin as shown in Figure 4.

The linear sweep voltammetry in Figure 5, which has been obtained using the droplet cell, has been used to present the electrochemical behaviour of the different zones in the sensitised and unsensitised Alloy 900. These results show that the electrochemical activity in the sensitised sample at 850 °C during 2 hours is higher than in the unsensitised sample, indicating the detrimental effect of the intermetallic phase precipitation. In the potential range where oxygen reduction occurs, the oxide film is partly reduced but an oxide film remains on the steel surface. According to the literature [112], oxygen reduction on polished surfaces is limited by the mass transport in the solution; however, on passivated surfaces, the oxygen reduction is limited by access of the oxygen to the metal surface and the electronic conductivity of the oxide film [112, 113]. Therefore, this result is indicative of the formation of a different passive film on the sensitised sample as opposed to that on the unsensitised sample.

Furthermore, according to the linear sweep voltammetry, the passivation current is higher in the case of the sensitised sample (Figure 5). A higher passivation current indicates a 'less-protective' passive film with higher electronic conductivity, this being due to the presence of areas depleted in alloying elements, notably chromium [53].

The Scanning Droplet cell also allows performing area scans in the samples investigated. As an example, Figure 6 shows the area scans carried out in an unsensitised and sensitised sample of Alloy 900.

These results show that the free potential in the sensitised sample (Figure 6b) is more negative than that obtained in the unsensitised sample (Figure 6a). This fact indicates that the free potentials of the unsensitised sample are more noble and, as a result the passive film on the

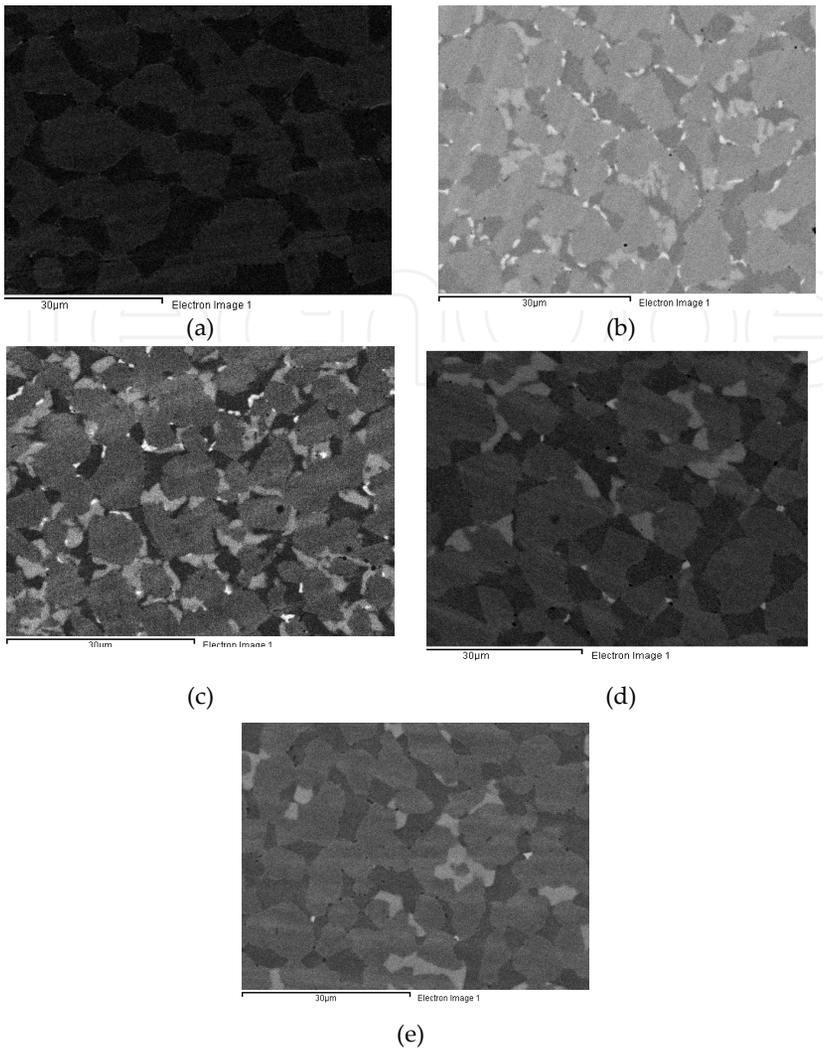

Figure 3. SEM images of the different Alloy 900 samples: a) unsensitised Alloy 900, b) sensitised Alloy 900 at 850 °C during 1 hour, c) sensitised Alloy 900 at 850 °C during 2 hours, d) sensitised Alloy 900 at 950 °C during 1 hour and e) sensitised Alloy 900 at 950 °C during 2 hours. Images were obtained with backscattered electrons.

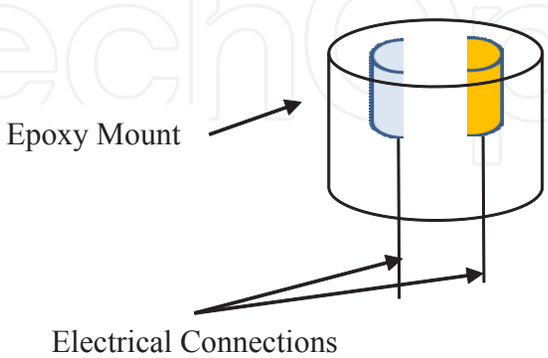

Figure 4. Schematic diagram of the working electrode tested by the different electrochemical techniques. Unsensitised sample on the rigth side.

http://dx.doi.org/10.5772/57204

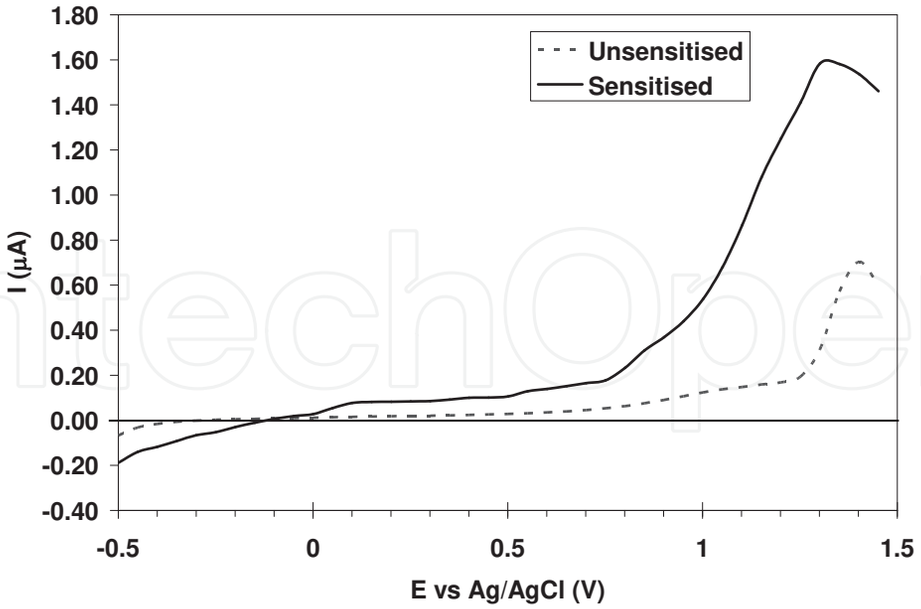

Figure 5. Linear sweep voltammetry of the sensitised and unsensitised samples of Alloy 900 carried out in the Scanning Droplet Cell.

sensitised sample presents a higher electrochemical activity, indicating a greater electronic conductivity of the passive film. Several authors [112, 114-116], proposed that the reduction pathway is influenced by the surface composition of the electrode and oxides have an important role to play in the oxygen reduction kinetics. A homogeneous mixture of chromium oxide and hydroxide constitutes a barrier to oxygen reduction, whereas no diffusion barrier is observed when the surface is only partially covered with a non-reducible chromium oxide [117]. Therefore, any chromium depleted areas formed in the sensitised alloy can lead to the formation of a more conductive passive film that promotes higher oxygen reduction on the electrode surface.

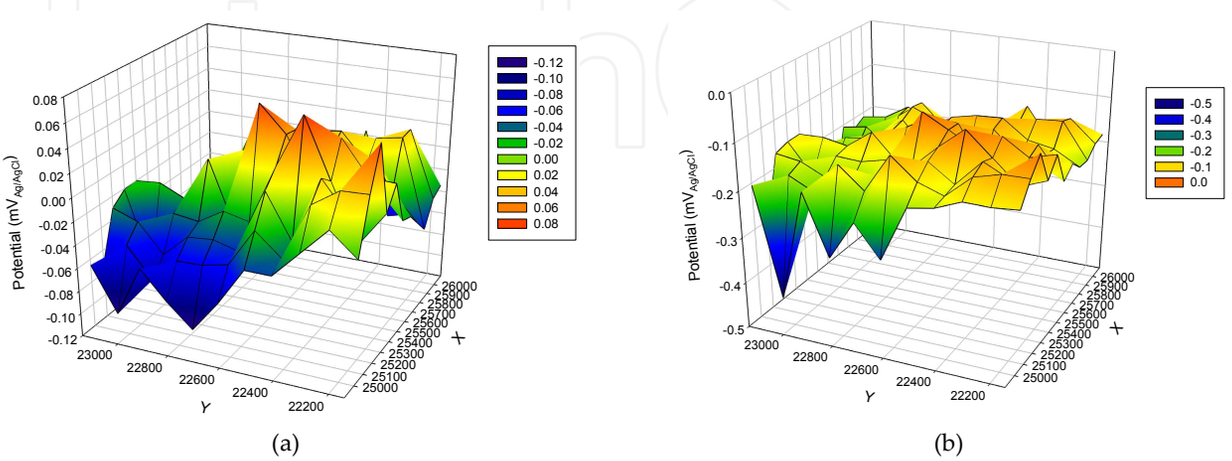

Figure 6. SDC area scans of the free potential in the (a) unsensitised and (b) sensitised sample of Alloy 900.

On the other hand, a similar behaviour can be observed if the different samples of Alloy 900 are analysed by means of the SECM technique. Figure 7 shows different line scans carried out on the samples of Alloy 900 after different states of sensitisation, notably, heated at 950 °C during 1 and 2 hours. It can be observed that the current registered with the tip over the sensitised sample is lower than over the unsensitised one. These differences in the oxygen reduction on one and another sample confirm the different electrochemical behaviour as a consequence of the heat treatment, which was also observed using the scanning droplet cell.

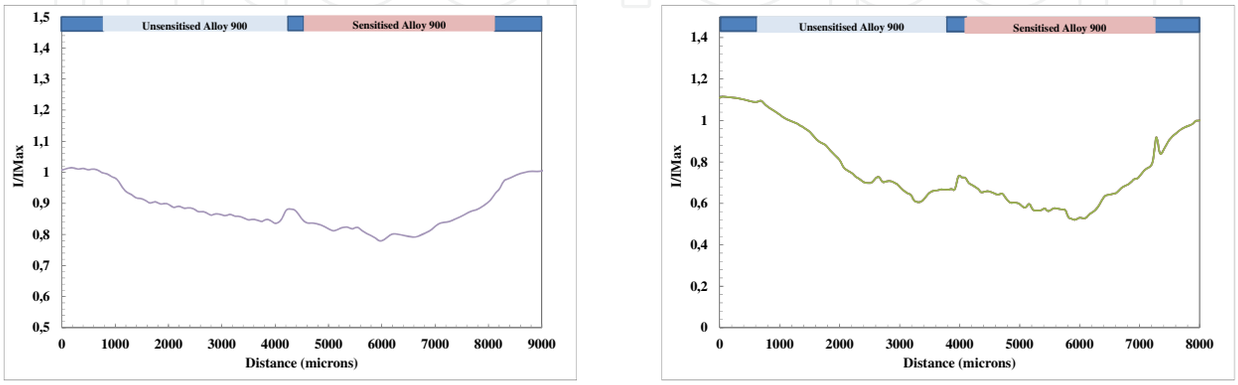

(a) 950 °C during 1 hour

(b) 950 °C during 2 hours

Figure 7. Line scans carried out over the Alloy 900 specimens in the 1 mM NaCl solution at 25 °C. The sensitised sample is on the right.

6.2. Welds in an austenitic stainless steel

Since approximately 20% of the pipeline construction costs are due to welding, coating, and subsequent maintenance to confirm their integrity [118], in the present study the application of the scanning electrochemical microscope to a welded type 316L tube will be shown. The most popular method for welding pipes is the shielded metal-arc process. However, the plasma arc welding technique is an alternative welding procedure which, thanks to its greater arc stability and energy concentration together with its deeper and narrower penetration, produces minimal detrimental residual stresses and distortion at the weld joints. This technique is an adequate welding method because its energy density is high. Microplasma arc welding (MPAW) is a variation of the plasma arc process with amperages between 0.05 and 15 A, used to weld thin pipelines [119].

The materials used to show the power of the SECM technique in order to analyse heterogeneous surfaces were tubes of type 316L SS and microplasma arc welded 316L type welded with filler alloy. Filler alloy was also 316L SS type. The tubes were 20 mm in length and 14 and 16 mm in inner and external diameter, respectively.

The MPAW process was performed manually using argon as backing gas, parameters of the welding process are shown in Table 3.

http://dx.doi.org/10.5772/57204

Welding process		Micro-plasma arc welding (MPAW)
Process type		Manual
Backing gas		Argon (99.9 %)
Flow rate		2.5 L/min
Plasma gas flow rate		6.5 L/min
Number of passes		2
Step 1	Current	11.3 A
	Voltage	20 V
	Welding speed	2.6 mm/s
Step 2	Current	13 A
	Voltage	20 V
	Welding speed	2.6 mm/s

Table 3. Welding parameters for the microplasma arc welding of the 316L SS type.

The materials were examined by light microscopy (LM) in order to estimate possible microstructural variations in them during the MPAW procedure. For this purpose, each material was cut lengthwise and covered in resin; then, the samples were wet abraded from 220 silicon carbide (SiC) grit to 4000 SiC grit. Then, they were polished with 1 and 0.3 micron alumina and were rinsed with distilled water and ethanol. Once the samples were polished, metallographic etching was carried out according to ASM International [120]. The etchant composition consisted of 10 mL of nitric acid, 10 mL of acetic acid, 15 mL of hydrochloric acid and 5 mL of glycerine. The samples were immersed in the etching solution during 90 seconds and then rinsed with distilled water and ethanol.

Figure 8 shows, the microstructure of the welded 316L SS. The microstructure of type 316L SS is a single-phase austenitic microstructure with equiaxed grains. A heat affected zone (HAZ) can be observed in Figure 8. The microstructure of this zone is characterized by an increase in grain size due to the fact that there is no transformation point at temperatures higher than room temperature [121]. Figure 8 also shows the microstructure of the weld zone (WZ). Usually, the WZ of austenitic stainless steels has a cast structure with the presence of 2-10 wt. % delta-ferrite in the austenite matrix [122]. Delta-ferrite presents two opposite phenomena: increasing its content causes a higher resistance to hot cracking [123, 124], but also reduces corrosion resistance due to the formation of a less stable passive film [125]. In Figure 8 it can be observed that the weld zone has columnar grains where delta-ferrite can be found. Alloys with especially low carbon contents (such as 316L SS type), to minimize susceptibility to sensitization during welding, present a greater tendency towards delta-ferrite stabilization [126]. The microstructure of delta-ferrite occurs in vermicular form. Vermicular morphology is typical of welds that solidify ferrite, followed by a subsequent formation of austenite involving the grains of ferrite until complete solidification. According to this fact, it is clearly observed that the microplasma arc welding process affects on the microstructure of the SS.

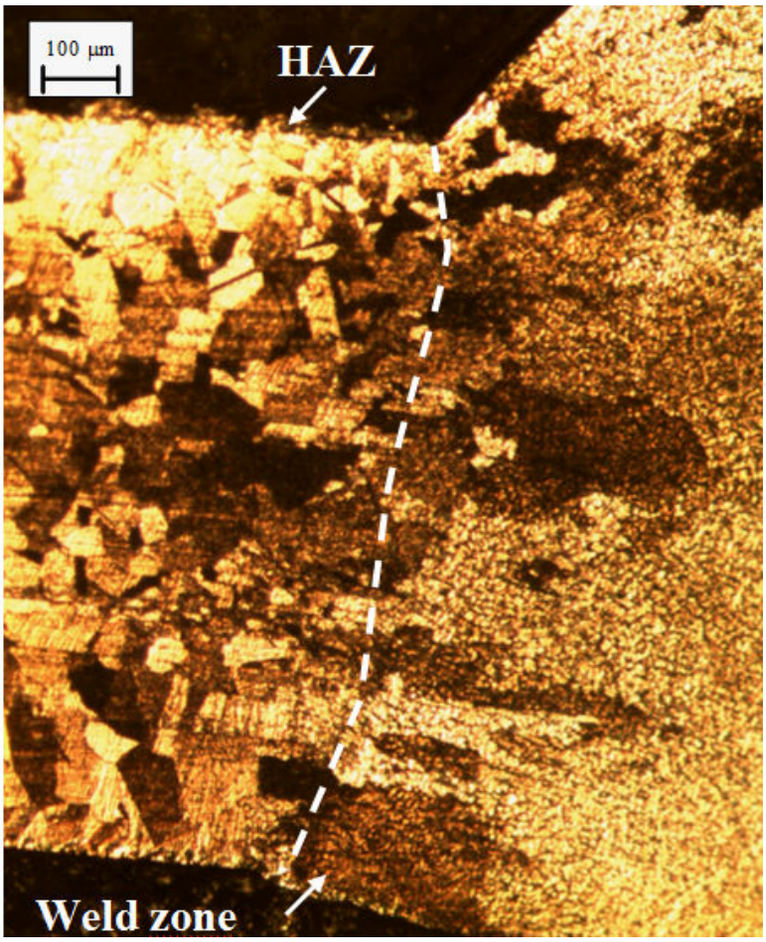

Figure 8. Microstructure of the microplasma arc welded 316L SS type [27].

Additionally, in order to know the influence of the microplasma arc welding technique on the mechanical properties of the stainless steel, Vickers microhardness measurements were carried out using a microhardness tester (Struers Duramin) with a diamond pyramid indenter at a load of 300 g and duration of 15 s [127]. Figure 9 shows the microhardness profiles across the base (non-welded) 316L SS and the microplasma arc welded 316L SS. As it is shown in the figure, the weld and the heat affected zones are softer than the base one. Since there is a positive correlation between hardness and strength; the higher the hardness values, the higher the strength. This fact indicates that the strength of the join decrease in the weld and heat affected zones [128].

In order to know how this microstructure and microhardness variations affect on the electrochemical behaviour of the stainless steel, SECM tests were performed. To carry out the scanning electrochemical measurements, the tubes were cut lengthwise and covered with resin; then, the samples were wet abraded from 220 silicon carbide (SiC) grit to 4000 SiC grit. Finally, they were rinsed with distilled water, ethanol and dried.

SECM tests were performed using a Sensolytics device connected to a bipotentiostat. The SECM was operated in "feedback mode". This technique measures a faradic current at the

http://dx.doi.org/10.5772/57204

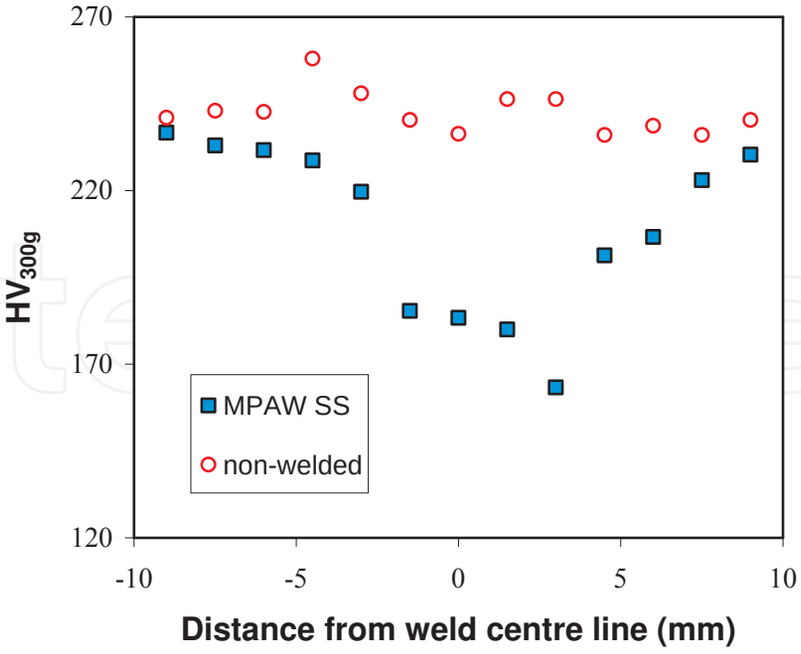

Figure 9. Microhardness profiles of the base and welded 316L SS.

microdisk, while the tip is scanned over the specimen surface. A platinum microelectrode tip of 25 μm in diameter was used as counter-electrode, and a silver/silver chloride (Ag/AgCl) 3M potassium chloride (KCl) microelectrode was used as reference electrode. The samples were immersed in a 35 g/L sodium chloride (NaCl) solution at 25 °C. All the tests were carried out in natural aerated solutions. Oxygen was used as the electrochemical mediator at the tip. The reduction of oxygen on the microelectrode was used to establish the height of the tip over the sample, and also to know the reactivity of the surface during the test. The cyclic voltammogram was recorded at a scan rate of 0.05 V/s from 0 $V_{Ag/AgCl}$ to -1.2 $V_{Ag/AgCl}$. The analysis of the data was used to choose the polarisation potential of the tip; in this study the experiments were performed at -0.6 $V_{Ag/AgCl}$.

Then approach curves (intensity vs distance from the surface of the sample) were performed in welded and base 316L SS. The progress of the dissolved oxygen reduction reaction was followed by setting the tip at -0.6 $V_{Ag/AgCl}$. Figure 10a shows the cyclic voltammetry of the welded alloy; where it can be clearly observed that at a potential of -0.6 $V_{Ag/AgCl}$ the detection of oxygen is under limiting current of oxygen reduction.

Figure 10b shows the approach curves of the base and welded SS. They show that the proximity of the tip to the specimen affects the diffusion of oxygen to the tip and hence the magnitude of the current. The drop in the current measured at the tip occurs at a shorter distance working with the welded 316L SS type than with the base one, indicating that the oxygen reduction reaction is higher over the SS surface in its welded state. Thus, there is a higher electrochemical activity on the welded alloy. This is due to the presence of chromium depleted regions and delta-ferrite originated in weldments [129, 130].

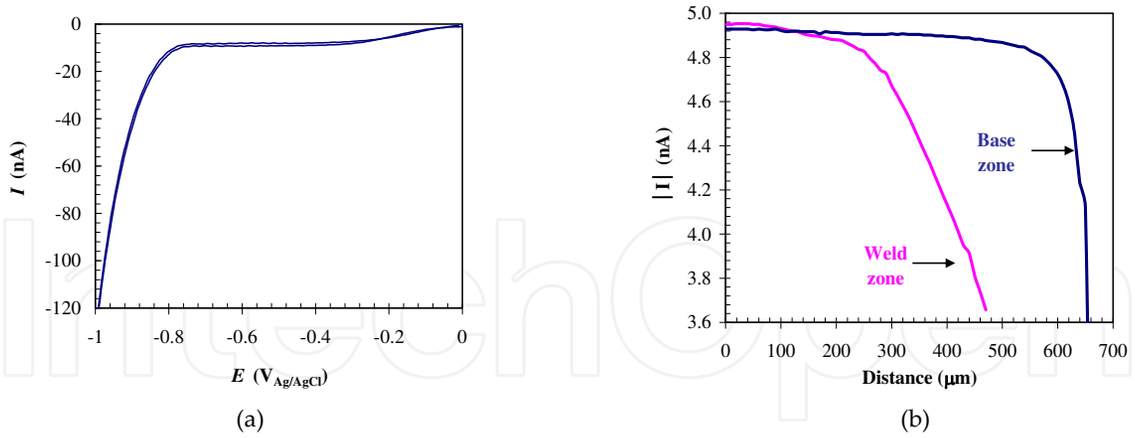

Figure 10. a) Cyclic voltammogram of the welded sample measured at the SECM tip, at the beginning of the test and (b) approach curves in the 35 g/L NaCl solution at 25 °C [84].

7. Conclusions

It can be concluded that SECM and SDC are powerful techniques that reveals substantial differences in the electrochemical activity of base and welded samples. These techniques can also contribute to the study of the galvanic effect in different materials, helping to the elucidation of the precursor sites for the pit formation. The use of localised techniques can complement the results obtained with conventional electrochemical techniques, leading to a better comprehension of the corrosion processes.

Acknowledgements

We wish to express our gratitude to MICINN (CTQ2009-07518) and to Universitat Politècnica de València (CEI-01-11).

Author details

R. Leiva-García, R. Sánchez-Tovar, C. Escrivà-Cerdán and J. García-Antón*

*Address all correspondence to: jgarciaa@iqn.upv.es

Univ. Politécnica de Valencia, Ingeniería Electroquímica y Corrosión (IEC), Dep. Ingeniería Química y Nuclear, Valencia, Spain

References

[1] Corrosion Costs and Preventive Strategies in the United States NACE (2002).

[2] Whitney, W. R. THE CORROSION OF IRON. Journal of the American Chemical Society 1903; 25(4), 394-406.

[3] Frumkin A., Damaskin B., Grigoryev N., Bagotskaya I. Electrochimica Acta 1974; 19 p. 69.

[4] Levich V. G., "Physico-Chemical Hydrodynamics," Academy of Sciences of the USSR Press (1959).

[5] Cobb HM. Steel Products Manual: Stainless Steels. Warrendale: Iron & Steel Society; 1999.

[6] Sedriks AJ. Corrosion Resistance of Stainless Steels and Nickel Alloys. In: Cramer SD, Covino BS Jr. (Eds.), Corrosion: Fundamentals, Testing and Protection. Vol. 13A. USA: ASM Handbook; 2003. 697-702.

[7] Hakiki N. E., Boudin S., Rondot B., Da Cunha Belo M. The electronic structure of passive films formed on stainless steels, Corrosion Science 1995; 37, 1809-1822.

[8] Wijesinghe T. L. S., Blackwood D. J.. Photocurrent and capacitance investigations into the nature of the passive films on austenitic stainless steels, Corrosion Science 2008; 50, 23-34.

[9] Lothongkum G., Chaikittisilp S., Lothongkum A. W.. XPS investigation of surface films on high Cr-Ni ferritic and austenitic stainless steels, Applied Surface Science 2003; 218, 203-210.

[10] Freire L., Carmezim M. J., Ferreira M. G. S., Montemor M. F.. The passive behaviour of AISI 316 in alkaline media and the effect of pH: A combined electrochemical and analytical study, Electrochimica Acta 2010; 55, 6174-6181.

[11] Almarshad A.I., Jamal D.. Electrochemical investigations of pitting corrosion behaviour of type UNS S31603 stainless steel in thiosulfate-chloride environment, Journal of Applied Electrochemistry 2004; 34, 67-70.

[12] Montañés M.T., Sánchez-Tovar R., García-Antón J., Pérez-Herranz V. The influence of Reynolds number on the galvanic corrosion of the copper/AISI 304 pair in aqueous LiBr solutions, Corrosion Science 2009; 51, 2733-2742.

[13] Honeycombe RWK, HKDH. Bhadeshia. Steels, Microstructure and Properties. Oxford: Butterworth Heinemann; 1995.

[14] Brinkman CR, Garvin HW. Properties of Austenitic Stainless Steels and Their Weld Metals: Influence of Slight Chemistry Variations. Vol. 679 Baltimore: ASTM special technical publication; 1979.

[15] Krauss J. Steels: Processing, Structure, and Performance. USA: ASM international; 2005.

[16] L. Antoni and B. Baroux: "Cyclic oxidation behaviour of stainless steels - appliation to the automotive exhaust lines", La Revue de métallurgie-CIT Février 2002; 178-188.

[17] Santacreu P.O., Sassoulas, H., Moser, F., Cleizergues, O., Lovato, G. Study of the thermal fatigue of stainless steels and its application to the life prediction of automotive exhaust line components. In: Skrzypek JJ., Hetnarski RB. (eds.). 3rd Int. Congress on Thermal Stresses: Thermal Stresses 1999, June 13-17, Cracow, Poland.

[18] Gunn RN. Duplex Stainless Steels: Microstructure, Properties and Applications. England: Abington publishing, Woodhead publishing Ltd in association with The Welding Institute; 1997.

[19] Alvarez-Armas I., Degallaix-Moreuil S. Duplex stainless steels. Great Britain; John Wiley and Sons Inc; 2009.

[20] Park C.J., Shankar Rao V., Kwon H.S. Effects of sigma phase on the initiation and propagation of pitting corrosion of duplex stainless steel, Corrosion 2009; 61, 76-83.

[21] Iacoviello F., Casari F., Gialanella S. Effect of "475°C embrittlement" on duplex stainless steel localized corrosion resistance, Corrosion Science 2005; 47, 909-922.

[22] Davis JR. Stainless Steels. Ohio: ASM International; 1994.

[23] Hemmingsen T., Hovdan H., Sanni P., Aagotnes N.O. The influence of electrolyte reduction potential on weld corrosion, Electrochimica Acta 2002; 47, 3949-3955.

[24] Shaikh H., Rao B.P.C., Gupta S., George R.P., Venugopal S., Sasi B., Jayakumar T., Khatak H.S. Assessment of intergranular corrosion in AISI Type 316L stainless steel weldments, British Corrosion Journal 2002; 37, 129-140.

[25] Lima A.S., Nascimento A.M., Abreu H.F.G., De Lima-Neto P. Sensitization evaluation of the austenitic stainless steel AISI 304L, 316L, 321 and 347, Journal of Materials Science 2005; 40, 139-144.

[26] Parvathavarthini N., Dayal R.K., Khatak H.S., Shankar V., Shanmungan V. Sensitization behaviour of modified 316N and 316L stainless steel weld metals after complex annealing and stress relieving cycles, Journal of Nuclear Materials 2006; 355, 68-82.

[27] Rao R.V.S., Parvathavarthini N., Pujar M.G., Dayal R.K., Khatak H.S., Kaul R., Ganesh P., Nath A.K. Improved pitting corrosion resistance of cold worked and thermally aged AISI type 316 L(N) SS by laser surface modification, Surface Engineering 2007; 23, 83-92.

[28] Stella J., Cerezo J., Rodríguez E. Characterization of the sensitization degree in the AISI 304 stainless steel using spectral analysis and conventional ultrasonic techniques, NDT & E International 2009; 42, 267-274.

[29] Leiva-García R., Muñoz-Portero M.J., García-Antón J. Evaluation of Alloy 146, 279, 900, and 926 sensitization to intergranular corrosion by means of electrochemical methods and image analysis, Corrosion Science 2009; 51, 2080-2091.

[30] Li S., Li L., Yu S.R., Akid R., Xia H.B. Investigation of intergranular corrosion of 316L stainless steel diffusion bonded joint by electrochemical potentiokinetic reactivation, Corrosion Science 2011; 53, 99-104.

[31] Sánchez-Tovar R., Montañés M.T., García-Antón J. Effect of different micro-plasma arc welding (MPAW) processes on the corrosion of AISI 316L SS tubes in LiBr and H_3PO_4 solutions under flowing conditions, Corrosion Science 2010; 52, 1508-1519.

[32] ASM Metals Handbook, Corrosion vol. 13, Corrosion of Weldments, ASM International, OH, 1992, pp. 771-838.

[33] ASM Specialty Handbook, Stainless Steels, Corrosion of Weldments, ASM International, OH, 1994, pp. 238-257.

[34] Garcia C., de Tiedra M.P., Blanco Y., Martin O., Martin F.. Intergranular corrosion of welded joints of austenitic stainless steels studied by using an electrochemical mini-cell. Corrosion Science 2008; 50, 2390-2397.

[35] Reclaru L., Lerf R., Eschler P.Y., Meyer J.M.. Corrosion behavior of a welded stainless-steel orthopedic implant Biomaterials 2001; 22, 269-279.

[36] Perren R.A., Suter T.A., Uggowitzer P.J., Weber L., Magdowski R., Böhni H., Speidel M.O.. Corrosion resistance of super duplex stainless steels in chloride ion containing environments: investigations by means of a new microelectrochemical method - I. Precipitation-free states. Corrosion Science 2001; 43, 707-726.

[37] Wloka J., Laukant H., Glatzel U., Virtanen S., Corrosion Properties of Laser Beam Joints of Aluminium with Zinc- Coated Steel. Corrosion Science 2007; 49, 4243-4258.

[38] Robert G. Kelly, John R. Scully, David Shoesmith, Rudolph G. Buchheit. Electrochemical Techniques in Corrosion Science and Engineering. Marcel Dekker: New York; 2003.

[39] Bard A. J., Faulkner L. R.. Electrochemical Methods. Fundamentals and Applications. John Wiley & Sons. Inc. New York; 2001.

[40] Enos D.G., Scribner L.L. The Potentiodynamic Polarization Scan. Technical Report 33. Solartron Instruments: UK; 1997.

[41] Baboian R., Electrochemical Techniques for Predicting Galvanic Corrosion, Galvanic and Pitting Corrosion - Field and Laboratory Studies, ASTM STP 576, American Society for Testing and Materials, 1976.

[42] Wolstenholme J., Inexpensive Zero-Resistance Ammeter for Galvanic Studies, British Corrosion Journal 1974; 9, No.2, 116-117.

[43] Macdonald D.D. Techniques for Characterization of Electrodes and Electrochemical Processes, Ed. by R. Varma and J.R. Selman, J. Wiley & Sons, New York, 1991, p. 515.

[44] Mansfeld F., Lorenz W.J. Techniques for Characterization of Electrodes and Electrochemical Processes, Ed. by R. Varma and J.R. Selman, J. Wiley & Sons, New York, 1991, p. 581.

[45] Szpak S. Techniques for Characterization of Electrodes and Electrochemical Processes, Ed. by R. Varma and J.R. Selman, J. Wiley & Sons, New York, 1991, p. 677.

[46] Electrochemical Impedance: Analysis and Interpretation, Ed. by J.R. Scully, D.C. Silverman and M.W. Kendig, ASTM, Philadelphia, 1993.

[47] Lasia A., Electrochemical Impedance Spectroscopy and Its Applications, Modern Aspects of Electrochemistry, B. E. Conway, J. Bockris, and R.E. White, Edts., Kluwer Academic/Plenum Publishers, New York, 1999, Vol. 32, p. 143-248

[48] Barker A L, Gonsalves M, Macpherson JV, Slevin CJ, Unwin P.R.. Scanning electrochemical microscopy: beyond the solid/liquid interface Analitical Chimica Acta 1999; 385, 223-40.

[49] Barker AL, Slevin CJ, Unwin PR, Zhang J 2001 Liquid Interfaces in Chemical, Biological, and Pharmaceutical Applications ed A G Volkov (New York: Marcel Dekker) p 283.

[50] Pu G, LongoML and BordenMA. Effect of microstructure on molecular oxygen permeation through condensed phospholipid monolayers Journal of American Chemical Society 2005; 127, 6524-5.

[51] Bard A J and Mirkin M V 2001 Scanning Electrochemical Microscopy (New York: Marcel Dekker).

[52] Bard, Allen; Fan, Kwak, Lev (1989). "Scanning Electrochemical Microscopy. An Introduction and Principles". Analytical Chemistry 61 (2): 132-138.

[53] Leiva-García R., Akid R., Greenfield D., Gittens J., Munoz-Portero M.J., García-Antón J. Study of the sensitisation of a highly alloyed austenitic stainless steel, Alloy 926 (UNS N08926), by means of scanning electrochemical microscopy Electrochimica Acta 2012; 70, 105-111.

[54] Arjmand F., Adriaens A.. Investigation of 304L stainless steel in a NaCl solution using a microcapillary electrochemical droplet cell: Comparison with conventional electrochemical techniques Electrochimica Acta 2012; 59, 222-227.

[55] Rees N.V., Compton R.G.. Hydrodynamic microelectrode voltammetry Russian Journal of Electrochemistry 2006; 44, 368-389.

[56] Bozek R.. Application of Kelvin Probe Microscopy for Nitride Heterostructures Acta Physica Polonica A 2005; 108, 541-554.

[57] Zisman W A 1932 A new method of measuring contact potential differences in metals Rev. Sci. Instrum. 3 367.

[58] Baikie et al, 'Work Function study of rhenium oxidation using an ultra-high vacuum scanning Kelvin probe, Journal of Applied Physics 2000; 88, 4371.

[59] Kelvin L, Fitzgerald G and Francis W Contact electricity of metals Phil. Mag. 1898; 46, 82.

[60] Christmann K, Ertl G and Pignet T Adsorption of hydrogen on a Pt(111) surface Surface Science 1976; 54, 365.

[61] Moores B., Simons J., Xu S., Leonenko S. Kelvin probe force microscopy in application to biomolecular films: Frequency modulation, amplitude modulation, and lift mode. Ultramicroscopy 2010; 110, 708-711.

[62] Nonnenmacher M, Boyle OMP, Wickramasinghe H.K. Kelvin probe force microscopy Applied Physic Letters 1991; 58, 2921.

[63] Weaver JMR, Abraham DW High resolution atomic force microscopy potentiometry Journal of Vacuum Science and Technology B 1991; 9, 1559-1561.

[64] Barth C., Hynninen T., Bieletzki T., Henry C.R., Foster A.S., Esch F., Heiz U. AFM tip characterization by Kelvin probe force microscopy. New Journal of Physics 2010; 12, 093024.

[65] Isaacs, H. S., Applications of current measurement over corroding metallic surfaces. Progress in Clinic Research 1986; 210, 37-44.

[66] SVP100 Manual, Version 1.23, Uniscan Instruments Ltd., Sigma House, Buxton, UK, SK17 9JB.

[67] Hughes M.C., Parks J.M. "An AC Impedance Probe as an indicator of corrosion and defects in polymer/metal substrate system", in Corrosion Control by Organic Coatings, Henry Leidheiser Jr., Editor, p. 45-50, NACE, Houston, Texas (1981).

[68] Lillard R.S., Moran P.J., Isaacs H.S., Method for Determining the AC Current Distribution at an Electrochemical Interface and Generating Local Impedance Data. Journal of Electrochemical Society 1992; 139, 1007-1012.

[69] Mierisch A.M., Yuan J., Kelly R.G., Taylor S.R., 'Probing Coating Degradation on AA2024-T3 Using Local Electrochemical and Chemical Techniques', Journal of Electrochemical Society, 1999; 146, 4449.

[70] Annergren I., Thierry D., F. Zou, Localized Electrochemical Impedance Spectroscopy for Studying Piting Corrosion on Stainless Steels" Journal of Electrochemical Society 1997; 144, 1208.

[71] Kinlen P.J., Menon V., Ding Y.. A Mechanistic Investigation of Polyaniline Corrosion Protection Using the Scanning Reference Electrode Technique. Journal of The Electrochemical Society 1999; 146, 3690-3695.

[72] Liu C., Bi Q., Leyland A., Matthews A.. An electrochemical impedance spectroscopy study of the corrosion behaviour of PVD coated steels in 0.5 N NaCl aqueous solution: Part II. EIS interpretation of corrosion behaviour. Corrosion Science 2003; 45 1257-1273.

[73] Akid R., Hovsepian P., Kok, Y.N. Tribocorrosion testing of stainless steel (SS) and PVD coated SS using a modified scanning reference electrode technique. Wear 2005; 259, 1472-1481.

[74] Simoes A.M., Battocchi D., Tallman D.E., Bierwagen G.P.. SVET and SECM imaging of cathodic protection of aluminium by a Mg-rich coating.Corrosion Science 2007; 49, 3838-3849.

[75] Simoes A.M., Battocchi D., Tallman D.E., Bierwagen G.P. Assessment of the corrosion protection of aluminium substrates by a Mg-rich primer: EIS, SVET and SECM study. Progress in Organic Coatings 2008; 63, 260-266.

[76] Souto R.M., Gonzalez-Garcia Y., Gonzalez S., Burstein G.T.. Damage to paint coatings caused by electrolyte immersion as observed in situ by scanning electrochemical microscopy. Corrosion Science 2004; 46, 2621-2628.

[77] Souto R.M., Gonzalez-Garcia Y., Gonzalez S., Burstein G.T.. Imaging the Origins of Coating Degradation and Blistering Caused by Electrolyte Immersion Assisted by SECM. Electroanalysis 2009; 21, 2569-2574.

[78] Karavai O.V., Bastos A.C., Zheludkevich M.L., Taryba M.G.,. Lamaka S.V, Ferreira M.G.S.. Localized electrochemical study of corrosion inhibition in microdefects on coated AZ31 magnesium alloy. Electrochimica Acta 2010; 55, 5401-5406.

[79] Oglea K., Morel S., Jacquet D.. Observation of Self-Healing Functions on the Cut Edge of Galvanized Steel Using SVET and pH Microscopy. Journal of The Electrochemical Society 2006; 153 1, B1-B5.

[80] Sinebryukhov S.L., Gnedenkov A.S., Mashtalyar D.V., Gnedenkov S.V.. PEO-coating/substrate interface investigation by localised electrochemical impedance spectroscopy. Surface & Coatings Technology 2010; 205, 1697-1701.

[81] McMurray H.N., Williams G., O'Driscoll S.. Chromate Inhibition of Filiform Corrosion on Organic Coated AA2024-T3 Studied Using the Scanning Kelvin Probe. Journal of The Electrochemical Society 2004; 151-7, B406-B414.

[82] Ruhlig D., Gugel H., Schulte A., Theisen W., Schuhmann W.. Visualization of local electrochemical activity and local nickel ion release on laser-welded NiTi/steel joints using combined alternating current mode and stripping mode SECM. Analyst, 2008; 133, 1700-1706.

[83] Jayaraj, J.; Mudali, U. Kamachi. Electrochemical Activity at the Interface of Dissimilar Explosive Joint of Stainless Steel with Zircaloy by Scanning Electrochemical Microscopy. Journal of Advanced Microscopy Research 2012; 7, 214-217.

[84] Sánchez-Tovar R., Montañés M.T., García-Antón J. Effects of microplasma arc AISI 316L welds on the corrosion behaviour of pipelines in LiBr cooling systems, Corrosion Science 2013; 73, 365-374.

[85] Benjamin P. Wilson, Justin R. Searle, Kirsi Yliniemi, T. Bryan Jones, David A. Worsley, H. Neil. McMurray. Investigation into the Effect of Spot Weld Electrode Life and Quality on the Corrosion Behavior of Galvanized Automotive Steel Using the Three-dimensional Scanning Vibrating Technique. ECS Transactions 2013; 50, 53-64.

[86] Eckhard K., Etienne M., Schulte A., Schuhmann W.. Constant-distance mode AC-SECM for the visualisation of corrosion pits. Electrochemistry Communications 2007; 9, 1793-1797.

[87] Gabrielli C., Joiret S., Keddam M., Portail N., Rousseau P., Vivier V.. Single pit on iron generated by SECM. An electrochemical impedance spectroscopy investigation. Electrochimica Acta 2008; 53, 7539-7548.

[88] Gonzalez-Garcia Y., Burstein G.T., Gonzalez S., Souto R.M.. Imaging metastable pits on austenitic stainless steel in situ at the open-circuit corrosion potential. Electrochemistry Communications 2004; 6, 637-642.

[89] Vuillemin B., Philippe X., Oltra R., Vignal V., Coudreuse L., Dufour L.C., Finot E.. SVET, AFM and AES study of pitting corrosion initiated on MnS inclusions by microinjection. Corrosion Science 2003; 45, 1143-1159.

[90] Krawiec H., Vignal V., Oltra R.. Use of the electrochemical microcell technique and the SVET for monitoring pitting corrosion at MnS inclusions. Electrochemistry Communications 2004; 6, 655-660.

[91] Ramana M. Pidaparti, Ronak R. Patel. Correlation between corrosion pits and stresses in Al alloys. Materials Letters 2008; 62, 4497-4499.

[92] Simoes A.M., Bastos A.C., Ferreira M.G., González-García Y., González S., Souto R.M.. Use of SVET and SECM to study the galvanic corrosion of an iron-zinc cell. Corrosion Science 2007; 49, 726-739.

[93] Jorcin J.B., Aragon E., Merlatti C., Pebere N. Delaminated areas beneath organic coating: A local electrochemical impedance approach. Corrosion Science 2006; 48, 2006 1779-1790.

[94] Liu Z.Y., Li X.G., Cheng Y.F. Understand the occurrence of pitting corrosion of pipeline carbon steel under cathodic polarization. Electrochimica Acta 2012; 60 259- 263.

[95] Snihirova D., Sviatlana V. Lamaka, M.F. Montemor, "SMART" protective ability of water based epoxy coatings loaded with CaCO3 microbeads impregnated with cor-

rosion inhibitors applied on AA2024 substrates, Electrochimica Acta 2012; 83, 439-447.

[96] Krawiec Halina, Vignal Vincent, Akid Robert. Numerical modelling of the electrochemical behaviour of 316 stainless steel based upon static and dynamic experimental micro-capillary based techniques: effects of electrolyte low and capillary sizeElectrochimica Acta 2008; 53 5252-5259.

[97] Gnefid S., Akid R. The Effects of Flow Rate on Pitting Corrosion of DSS2205. The European Corrosion Congress 2009, Nice (France).

[98] Shao Y., Jia C., Meng G., Zhang T., Wang F. The role of a zinc phosphate pigment in the corrosion of scratched epoxy-coated steel. Corrosion Science 2009; 51, 371-379.

[99] Yin Y., Niu L., Lu M., Guo W., Chen S. In situ characterization of localized corrosion of stainless steel by scanning electrochemical microscope. Applied Surface Science 2009; 255, 9193-9199.

[100] Liu X., Zhang T., Shao Y., Meng G., Wang F. Effect of alternating voltage treatment on the corrosion resistance of pure magnesium. Corrosion Science 2009; 51, 1772-1779.

[101] Fu A.Q., Cheng Y.F.. Characterization of corrosion of X65 pipeline steel under disbonded coating by scanning Kelvin probe. Corrosion Science 2009; 51 914-920.

[102] Fu A.Q., Cheng Y.F.. Characterization of corrosion of X70 pipeline steel in thin electrolyte layer under disbonded coating by scanning Kelvin probe. Corrosion Science 2009; 51, 186-190.

[103] Cavalcoli D, Cavallini A, Rossi M. Surface contaminant detection in semiconductors using noncontacting techniques. Journal of the Electrochemical Society 2003; 150, G456-G460.

[104] Borgwarth K., Ebling D., Heinze J.. Applications of scanning ultra micro electrodes for studies on surface conductivity. Electrochimica Acta 1995; 40, 1455-1460.

[105] Zin I.M., Lyon S.B., Hussain A.. Under-film corrosion of epoxy-coated galvanised steel an EIS and SVET study of the effect of inhibition at defects. Progress in organic coatings 2005; 52, 126-135.

[106] Kiran B. Deshpande. Numerical modeling of micro-galvanic corrosion. Electrochimica Acta 2011; 56, 1737-1745.

[107] Berger F., Delhalle J., Mekhalif Z.. Hybrid coating on steel: ZnNi electrodeposition and surface modification with organothiols and diazonium salts. Electrochimica Acta 2010; 53, 2852-2861.

[108] Zhang G.A., Cheng Y.F.. Micro-electrochemical characterization of corrosion of welded X70 pipeline steel in near-neutral pH solution. Corrosion Science 2009; 51, 1714-1724.

[109] Akid R., Roffey P, Greenfield D., Guillen D.. Application of scanning vibrating electrode technique (SVET) and scanning droplet cell (SDC) techniques to the study of weld corrosion. Local Probe Techniques for corrosion research. 978-1-4200-5405-7 (CRC Press): 2013.

[110] Kim J.S., Kwon H.S. Effects of tungsten on corrosion and kinetics of sigma phase formation of 25% chromium duplex stainless steels. Corrosion 1999; 55 (5) 512-521.

[111] Park C.J., Kwon H.S., Lohrengel M.M. Micro-electrochemical polarization study on 25% Cr duplex stainless steel. Materials Science and Engineering A, 2004; 372 180-185.

[112] Le Bozec N., Compère C., L'Her M., Laoueman A., Costa D., Marcus P.. Influence of stainless steel surface treatment on the oxygen reduction reaction in seawater. Corrosion Science 2001, 43(4) 765-786.

[113] Okuyama M., Haruyama S., The cathodic reduction of oxygen on stainless steels in a neutral solution. Corrosion Science 1990; 31, 521-526.

[114] Gojkovic S.L.J., Zecevic S.K., Obradovic M.D., Drazic D.M.. Oxygen reduction on a duplex stainless steel. Corrosion Science 1998; 40(6) 849-860.: 2013.

[115] Calvo E.J., Schiffrin D.J.. The reduction of hydrogen peroxide on passive iron in alkaline medium. Journal of Electroanalytical Chemistry 1984; 163, 257-275.

[116] Zecevic S., Drazic D.M., Gojkovic S.L. Journal of Electroanalytical Chemistry 1989; 265, 179.

[117] Ramasubramanian N., Preocanin N., Davidson R.D.. Analysis of Passive Films on Stainless Steel by Cyclic Voltammetry and Auger Spectroscopy Journal of Electrochemical Society 1985; 132, 793-798.

[118] Mohammadi F., Eliyan F.F., Alfantazi A. Corrosion of simulated weld HAZ of API X-80 pipeline steel, Corrosion Science 2012; 63, 323-333.

[119] Jiang Y., Xu B., Lu Y., Xiang Y., Liu C., Xia D. Application prospects of plasma welding within remanufacturing engineering. 4th World Congress on Maintenance 2008: conference proceedings, November 24-26, Haikou, Hainan, China.

[120] Vander Voort G.F. Metallography: Principles and Practice. New York: ASM International; 1999.

[121] Conde y Santiago G. Aceros inoxidables, refractarios y criogénicos (Stainless Steels, refractory and cryogenic). Madrid: INTERCIENCIA; 1971.

[122] Lu B.T., Chen Z.K., Luo J.L., Patchett B.M., Xu Z.H. Pitting and stress corrosion cracking behavior in welded austenitic stainless steel, Electrochimica Acta 2005; 50, 1391-1403.

[123] Patchett BM., Bringas J. The Metals Blue Book, Filler metals. USA: CASTI Publishing Inc. and American Welding Society (AWS); 1998.

[124] Lo I.-H., Tsai W.-T. Effect of heat treatment on the precipitation and pitting corrosion behavior of 347 SS weld overlay, Materials Science Engineering A 2003; 355, 137-143.

[125] Pujar M.G., Dayal R.K., Gill T.P.S., Malhortra S.N., Role of delta-ferrite in the dissolution of passive films on the austenitic stainless-steel weld metals, Journal of Materials Science Letters 1999; 18, 823-826.

[126] Vander Voort GF., James HM., Wrought Stainless Steels, Metallography and Microstructure. Vol. 9. USA: ASM International; 1992.

[127] ASTM E-384, Standard Test Method for Microindentation Hardness of Materials. ASTM International; 1999.

[128] De Lima-Neto P., Farias J.P., Herculano L.F.G., de Miranda H.C., Araújo W.S., Jorcin J.B., Pébère N. Determination of the sensitized zone extension in welded AISI 304 stainless steel using non-destructive electrochemical techniques, Corrosion Science 2008; 50, 1149-1155.

[129] Olsson C.-O. A., Landolt D. Passive films on stainless steels: chemistry, structure and growth, Electrochimica Acta 2003; 48, 1093-1104.

[130] White W. E. Observations of the influence of microstructure on corrosion of welded conventional and stainless steels, Materials Characterization 1992; 28, 349-358.